ORCA
ULTRA HEAVY-LIFT AIRSHIP

TODD ERICKSON | SINA GOLSHANY | SEAN KEIL | JORGE MONTOYA | BUGRA TURAN

JOHN F. WINKLER PH.D.

UNIVERSITY OF SOUTHERN CALIFORNIA

VITERBI SCHOOL OF ENGINEERING

MAY 2011

TABLE OF CONTENTS

1.0 ABSTRACT

This project explores the feasibility of a heavy lift hybrid airship for the purposes of transporting commercial and military cargo. A hybrid airship is a vehicle that combines the aerodynamic lift with the buoyancy of a lighter than air gas in order to create substantial amounts of lift at very low speeds. Flying at a lower speed causes the vehicle to require much less thrust at cruise therefore substantially reducing the fuel burn. As the fuel costs are increasing and presently form a major part of cash operating cost of any air vehicle, this reduction in fuel burn will entail a significant reduction in the cash operating cost of the vehicle and increased profit margins for the operators.

The goal of this project is to define a methodology and accordingly design a fully integrated hybrid airship to satisfy the performance requirements set by a request for proposal authored by the AIAA while creating a design fully compatible with present day infrastructure. In perusing this goal, various method of design space exploration have been adopted and modified to suit the configuration of a hybrid airship. Tools such as computational fluid dynamics analysis, numerical multidisciplinary optimization, and computer aided design are utilized to address different issues encountered throughout the project development. The final configuration is a vehicle with 548 meters length, 80 meters (262 ft.) span and 81 meters (265 ft.) height. Maximum takeoff weight is approximately 2.6 million pounds, and the maximum payload capacity is 1.2 million pound. The fuel burn of the craft over the mission profile is approximately 100,000 lb., which results in a reduction of fuel cost per ton-nautical mile by a factor of 22 compared to a Boeing 747-8F.

2.0 NOMENCLATURE

b_{env}	Envelope span
$C_{L,env}$	Lift coefficient, envelope
C_L	Lift Coefficient
$C_{D0,env}$	Zero-lift drag coefficient, envelope
$C_{D,env}$	Drag coefficient, envelope
D_{env}	Drag of the envelope
F_a	Fraction of the total lift that is achieved aerodynamically
F_{aw}	Fraction of F_a that is achieved using wings
g	Acceleration due to gravitational potential.
h_{tube}	Distance from keel beam to support cables
K_{env}	Induced drag factor
l_f	Length of the forward keel beam
l_b	Length of aft keel beam
L_{env}	Lift of the envelope
L_{He}	Buoyant lift from Helium
$M_{(x)}$	Bending moment on the keel beam
ϱ_{He}	Density of Helium
ϱ_{air}	Density of Air
R_{tube}	Radius of the keel beam
σ_{max}	Maximum Allowable Stress
t/c_{env}	Envelope thickness to midline chord ratio
t_{tube}	Thickness of the keel beam
W_e	Airship empty weight

ACLS	Air Cushion Landing System
AIAA	American Institute of Aeronautics and Astronautics
AMP	Airplane Market Price
APU	Auxiliary Power Unit
CAD	Computer Aided Design
CFD	Computational Fluid Dynamics
DATCOM	USAF Stability and Control Data Compendium
DOC	Direct Operating Costs
DOCflt	Flying Direct Operating Costs
HCS	Heaviness Control System
MTOW	Maximum takeoff weight
NACA	National Advisory Committee for Aeronautics
RFP	Request For Proposal
TEU	Twenty-foot Equivalent Unit
VTOL	Vertical takeoff and landing

3.0 INTRODUCTION

There are currently two main methods for overseas heavy cargo transportation: airfreight and cargo ships. Current market is dominated by waterborne transportation, which accounts for 99.6% of the total worldwide freight[1]. In addition, the energy efficiency (energy cost per dollar of gross output) of the transportation method plays a role. Transport by water, at 8.4% of the total gross output, is the second most efficient mode of transport. Air transport is least efficient, with 19.8% of the total as shown in Fig. 1.

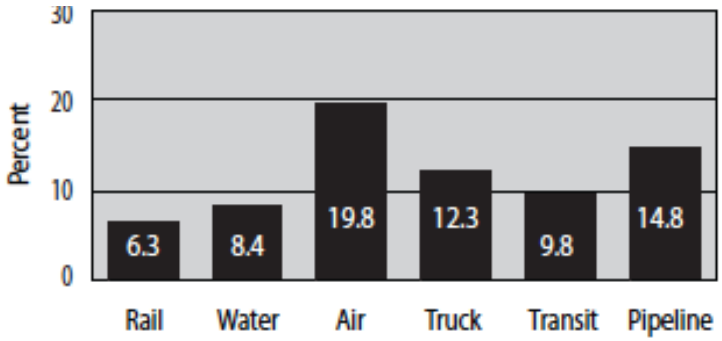

Figure 1. Energy Inputs as a percent of Gross Output by Mode, 2005 [2]

Both transportation methods described have certain advantages and disadvantages. Airfreight is fast but expensive, while ships are slow but cheap. For example, the Boeing 747-8F can deliver cargo 4,390 nmi in only 17 hours, but at a fuel cost of about $1.99/ton-nmi[3]. In comparison, a standard container ship travels the same distance in a very slow 170 hours, but is much cheaper at about $0.008/ton-nmi[4]. It is important to note that both methods require trucks, trains, or both between final destinations, which may increase the cost.

The previous evidence clearly shows a large gap between the fast -but expensive- and slow -but cheap- forms of cargo transportation. Thus, there is a pressing need to fill that gap with an alternative freight method that is relatively fast and low-cost. The goal of this paper is to present a highly detailed and fully integrated freight vehicle design capable of serving as that alternative.

A hybrid air vehicle accomplishes the objective by combining the aerodynamic lift of a lifting body, hull, or wings (as an airplane) and the efficient lighter-than-air buoyancy of a helium filled envelope (as a blimp or airship). The concept is nothing new. A hybrid aircraft was attempted as early as 1905, with the combination of an airship envelope with an airplane frame proposed by Alberto Santos Dumont. However, their feasibility and cost effectiveness as a mode of heavy cargo transport has been only realized in recent years, through significant advancements in materials, development tools and processes, and modern technology.

Through detailed analysis, an accurate model of a hybrid airship was derived that could fill the gap in heavy load transportation, as illustrated in Fig. 2.

Figure 2. The airship proposed (center) fills the large gap between air, sea, and rail cargo transport

4.0 Design Requirements

The American Institute of Aeronautics and Astronautics (AIAA) requests proposals each year for a comprehensive design of some type of aerospace vehicle. In the current year (2011) the request for proposal (RFP, Appendix I) entails the design of a hybrid air vehicle able to accomplish several goals and meet various general requirements. An outline of the requirements is shown in Table 1.

The hybrid airship is to have a payload capability of 1,200,000 lbs. By comparison, the Boeing 747-8F has a total payload capability of 308,000 lb.[5]. The increase in payload capacity by about a factor of 4 enables the airship to remain a viable alternative to the much quicker freightliners while reducing costs through greater fuel efficiency.

Range is an important factor for a cargo vehicle, since increasing the distance to which cargo can be carried often reduces the cost of transportation. In addition, commercial freight carriers, such as FedEx, UPS, or DHL, transport cargo overseas in a relatively short amount of time. Also, many military missions would require the transport of heavy loads to distant battle zones. The RFP requires the hybrid air vehicle to have a range of at least 6,000 nmi, consistent with commercial and military customer needs, while maintaining cost efficiency. As a comparison, the 747-8F has a range of 4,390 nmi[3].

Another great advantage of the hybrid air vehicle requested by AIAA is its ability to land and take off from virtually any reasonably level surface. This is accomplished through the use of an air cushion landing system (ACLS), integrated beneath the large aircraft. The military would especially appreciate the option to load and unload heavy payloads from almost anywhere, including remote battlefields, deserts, harbors, marshes, or snow covered surfaces.

Other performance parameters as required by the RFP or defined during the design process, such as endurance, cruise speed, and cruise altitude, are considered reasonable and incorporated into the design of ORCA.

Table 1. Summary of design requirements

Item	Requirement
Payload	1,200,000 lb.
Range	6,000 nmi
Endurance	3 days
Cruise Speed	90 KEAS
Cruise Altitude	10,000 ft.
Landing System	Air Cushion Landing System
Airport Compatibility	Maximize

5.0 DESIGN METHODOLOGY

As the initial research performed indicated, there is a general lack of methods for estimating the aerodynamic characteristics of blunt low aspect ratio lifting bodies, very large Reynolds number friction drag coefficients, structural weight estimation, and system integration general practices for very large hybrid airships. In order to explore the configuration possibilities with sufficient accuracy, and to produce an optimum design, a design methodology was defined.

The main numerical tool used in the design process is a Microsoft Excel-based numerical optimization code, which formulates a configuration that satisfies the performance requirements while minimizing either the direct operating cost (DOC) or fuel burn of the aircraft. The code includes multiple modules that are interconnected and are driven by a hill-climbing algorithm that varies the geometry of the craft until chosen parameter is optimized and all the performance criteria are met. As the vehicle had to be designed to be fully compatible with existing infrastructure, later research determined that the overall span of the vehicle has to be less to 80 meters (262 ft.) to maintain compatibility with taxiways in airports. This limits the full extent of external geometries to be explored. The basic configuration concept evolution is discussed in more detail in section 6.0 of this document. It is notable that in the process of designing the ORCA airship, typical graphical methods of constructing a sizing chart or carpet plot are not utilized, in turn, the numerical iteration eliminates the need for sizing charts and carpet plots to aid the decision making, although they can be constructed if needed.

In the area of aerodynamics, initial exploratory CFD analysis indicated that the typical equations for estimating the drag produced by a body have very large errors in the results they produce, compared to the CFD results. Even the equations cited by U.S. Air force DATCOM[1] were unable to predict the drag coefficient of a low aspect ratio lifting body with any reasonable accuracy. It was decided to prescribe corrections to the typical drag equations, and use them in the main code for the optimization and performance evaluation. The process of obtaining the corrections for the friction and induced drag of the low aspect ratio lifting body is presented in section 9.0.

Computing the weight of the craft also presented difficulties. As an analytic method for computing the weight for a low pressure thin walled envelope could not be obtained, a substitute structural sizing and weight estimation method was adopted, which is explained in full detail in the envelope structure and weight justification section in this report. Weight of the gondola, wing, propulsion and sub-systems were computed using various methods presented by Roskam[6].

As a hybrid airship relies heavily on buoyancy to generate lift, its flight mechanics are significantly different than those of a typical aircraft. The performance equations derived for typical aircraft do not apply. A survey of literature indicated multiple sources, such as Zhang et al[7], that drive and present corrected performance equations for hybrid airships. These methods were adopted and utilized in the main sizing and optimization tool to evaluate the performance of the vehicle, assuring the meeting of all requirements. Finally, the cost analysis methodology presented by Roskam[8] was adopted and utilized to estimate the unit cost and operational cost of the aircraft. This method makes numerous assumptions including the difficulty of the detailed design, manufacturing, and complexity of the materials utilized and the experience level of the company undertaking the design and manufacturing efforts.

[1] Recommended in a conversation by Dr. Daniel P. Raymer.

6.0 TRADE-OFFS AND DESIGN EVOLUTION

Even when the requirements given by the RFP are very specific with regards to the nature and the performance of the vehicle designed, the design of all of the main components consisted on a selection and iteration process, as described in the previous section. For each component or system, many possible design solutions were compared and evaluated to select the most suitable for the current application. Once the type of component or solution to be implemented was selected, an iterative optimization process was carried until the optimum results were obtained. This section summarizes the main trade-offs and optimizations made, as well as the evolution of the design from its beginning to its final result. Table 2 summarizes the components and systems that underwent trade-offs and optimization during their design. Fig. 3 summarizes the evolution of the design.

Table 2. Trade-offs and Optimized Item

Item	**Maximum Span of Envelope/Wings (Sections 4.0 and 15.0)**			
Options Considered	A wide range of spans was considered.			
Selected/Reasons	80 m (262 ft.) was selected as the maximum span for the airship to maximize compatibility with current airport infrastructure, most significantly, the taxi ways.			
Item	**Aerodynamic Lift Fraction of Total Lift (Section 9.0)**			
Options Considered	A range from 0 to 100 percent was considered			
Selected/Reasons	From the optimization tool, a value of 10% was determined to be optimum to minimize fuel consumption.			
Item	**Fraction of Envelope Aerodynamic Lift of Total Aerodynamic Lift (Section 9.0)**			
Options Considered	A range of values from 0 to 100 percent was considered and evaluated using the optimization tool developed.			
Selected/Reasons	From the optimization tool, a value of 10% was determined to be optimum to minimize fuel consumption.			
Item	**Envelope Profile (Sections 8.0 and 9.0)**			
Options Considered	Modified NACA 67-xxx airfoils with thicknesses ranging from 10 to 15 percent.			
Selected/Reasons	From the optimization tool, a thickness of 12.5% was determined to be optimum.			
Item	**Cargo bay Dimensions (Section 8.0)**			
Options Considered	All the possible payload dispositions were evaluated and the surface area measured.			
Selected/Reasons	The dimensions of 2x6x8 TEU containers were selected as they minimized surface area per unit volume.			
Item	**Propulsion System (Section 8.0)**			
Options Considered	Turbofans	Turbojets	**Turboprop**	Reciprocating
Selected/Reasons	Turbo Prop engines were selected given their high efficiency at the range of speeds and power of the application.			
Item	**Envelope Exterior Structure Materials (Section 11.0)**			
Options Considered	Aluminum		**Carbon Fiber Composites**	
Selected/Reasons	Composites were selected given their low weight and high strength.			

Table 2 (Contd.) Trade-offs and Optimized Item

Item	**ACLS Skirt type (Section 8.0)**			
Options Considered	Bag	Rigid Wall	**Bag and Finger**	
Selected/Reasons	The bag and finger type of skirt was selected for its high efficiency and for being the most widely used in current applications.			
Item	**ACLS distribution (Section 8.0)**			
Options Considered	**Single Cushion**	Two-Cushion	Three-Cushion	Four-Cushion
Selected/Reasons	A single cushion was selected to maximize its area and stability while minimizing power required.			
Item	**ACLS Power Source (Section 8.0)**			
Options Considered	Dedicated Engines	Mechanical from Main	Conventional Electric	**Superconducting**
Selected/Reasons	The high power density and current stage of development make of superconducting engine and generators an alternative for aerospace applications, increasing efficiency and significantly reducing weight compared to the other alternatives.			
Item	**Heaviness Control System Type (Section 8.0)**			
Options Considered	High Pressure Air	High Pressure Helium	Ballast	**Low Pressure Helium and Air**
Selected/Reasons	Only type capable of performing the task in an efficient manner.			
Item	**HCS Power Source (Section 8.0)**			
Options Considered	**Dedicated Engines**	Mechanical from Main	Conventional Electric	Superconduction
Selected/Reasons	The necessity of having additional engines as APU was combined with the requirement of power for the HCS.			

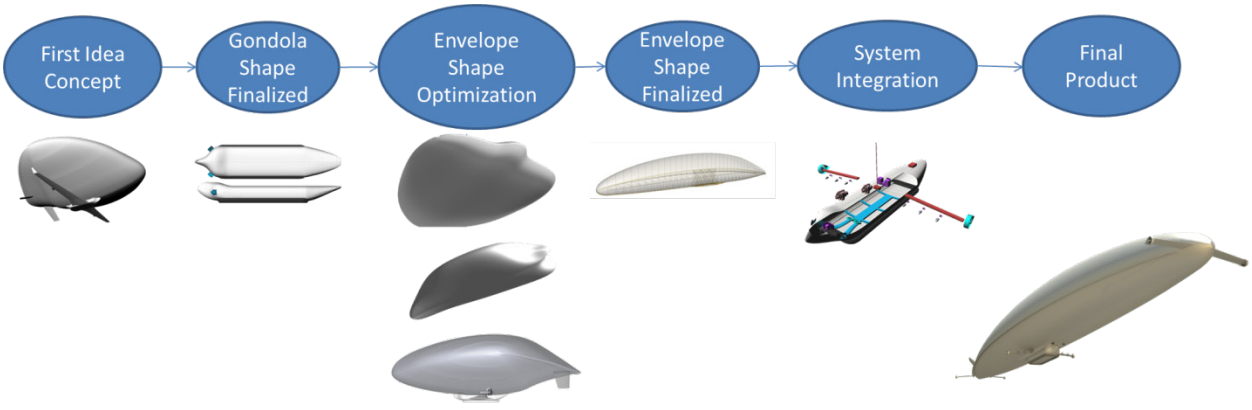

Figure 3. Design Evolution of ORCA

7.0 SIZING

The sizing of an ultra-heavy lift hybrid airship differs from that of a conventional airplane. Some of the differences include: greatly different weights, the presence of buoyant lift, and nonconventional geometries. Additionally, this design features novel concepts which also serve to distinguish it from the sizing and analysis of a traditional airplane. In order to address these differences, an integrated and automated sizing tool was created using Microsoft Excel.

The tool consisted of many interconnected worksheets, each acting as its own module. These sheets included: Geometry and Aerodynamics, Weight, Wind, ACLS Weight, Fuselage and Wing Weight, Performance and Fuel, Propulsion, Atmosphere, Cost, and Trade. These modules will be further described in this section.

Geometry and Aerodynamics

The Geometry and Aerodynamics sheet serves as one of the main convergence points in the tool. It uses the amount of lift required, F_a, F_{an}, b_{env}, t/c_{env}, the geometric parameters of the wings, and the atmospheric conditions to determine the shape and size of the envelope, the size of the wings, and the overall lift and drag characteristics of the airship.

Weight

The Weight sheet serves as the other main convergence point of the tool. It takes any weight data from the other sheets and adds it together to get the W_e and MTOW, and holds all of the different weight components together for easy comparison.

Wind

The wind sheet calculates the effect of side winds on the large envelope portion of the airship, and is used to size the heaviness control system. The amount of resistance the ground provides by different ground materials is analyzed using methods from Wong [9]. The bottom of the airship is modeled as a tracked vehicle in 100% slip. This is the off-road equivalent of the coefficient of kinetic friction.

ACLS Weight

The ACLS weight sheet calculates the power requirements and weight of the Air Cushion Landing System based upon the fuselage geometry and the maximum apparent weight of the airship during taxi.

Fuselage and Wing Weight

The fuselage and wing weight sheet calculates the weight of both the fuselage and wing based upon their geometry. In order to provide this, it also sizes the envelope requirements of the heaviness control system, and the main keel beam system of the airship.

Performance and Fuel

The performance and fuel sheet gains the fuel required for both the cruise and endurance missions by using the inverse of the hybrid airship equivalents of the Breguet range equation.

Propulsion

The propulsion sheet calculates the maximum power required, and therefore the number of engines required for the airship by taking into account takeoff, initial climb, max cruise, and top of climb. It also calculates the weight of this propulsion system.

Atmosphere

The atmosphere sheet calculates the atmospheric conditions at several key mission segments.

Cost

The cost sheet calculates the Research and Development, Manufacturing and Acquisitions, and Operating costs of the airship.

Trade

The trade sheet creates studies based upon the variation of F_a and F_{aw}.

Process

The sizing process begins with an MTOW. That weight is used by the Geometry and Aerodynamics sheet to get the geometric size of the airship by increasing the envelope volume until enough buoyant lift is achieved, and changing $C_{L,env}$ until enough aerodynamic lift is achieved. These sizes and initial weight are then used by all the other sheets to produce their respective results. These results include the new individual component weights, which are added together to get a new MTOW. This new MTOW is now used as the initial guess, and the process is repeated until the new MTOW is within 0.1% of the initial guess.

The tool also has the ability to optimize t/c_{env} by minimizing either fuel weight or DOC.

8.0 Configuration Description

The airship consists of three main structurally and functionally distinct elements (the envelope, the gondola, and the wing group), which will be described in this section. Other specific systems and their integration will be further described in section 10.0.

Envelope

The gas envelope is the element that contains the lifting gas (helium) that produces aerostatic lift. Historically, airship envelopes are usually classified according to their rigidity into non-rigid envelopes, semi-rigid envelopes and rigid envelopes. ORCA has a rigid envelope as the one used in Zeppelins and other largely successful airships throughout history. In this type of envelope, the shape is maintained by the use of a rigid structure and skin, in a fashion similar to that of airplane fuselages (semi-monocoque). The envelope surrounds multiple gas cells that contain helium, making it possible to change the volume and pressure of the lifting gas without affecting the shape of the envelope or its aerodynamic characteristics.

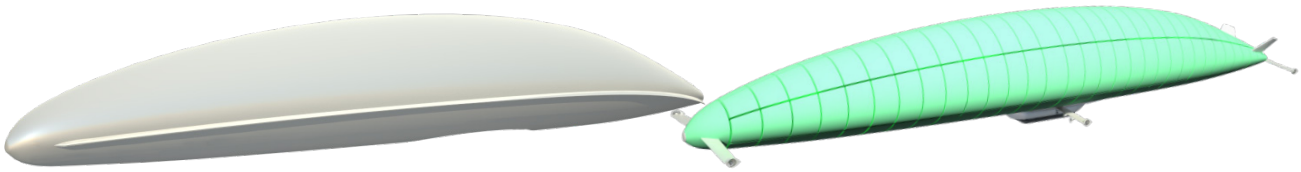

Figure 4. Gas envelope (left) and gas cells (right).

The tradeoffs and optimization of the vehicle for minimizing fuel burn resulted in an optimum static lift fraction of 0.9, making it necessary for the envelope to produce 90% of the total lift required in the form of aerostatic force. By applying basic aerostatic theory, the useful buoyancy (lift) obtained by some volume of helium can be obtained by applying Eqn. 1. Since the amount of lift required is known from the optimization tool, Eqn. 2 was derived to determine the required volume of helium to produce the necessary lift.

$$L_{He} = V_{He} * g * (\rho_{air} - \rho_{He}) \quad (1)$$

$$V_{He} = \frac{L_{He}}{g*(\rho_{air}-\rho_{He})} \quad (2)$$

Equation 2 was evaluated at both sea level and maximum cruise altitude (11,500 ft.) to guarantee that the envelope would produce enough aerostatic lift at both conditions. It was found that at cruise altitude the net available lift from the envelope is reduced given the relative change in densities of helium and air with altitude. For this condition, a volume of helium of 41.6×10^6 cubic feet is required to produce the necessary lifting force of 2.34×10^6 lbf.

As previously described, the requirement of maximizing compatibility with current airport infrastructure limits the maximum span of the envelope to 262 ft. Once this dimension was defined, an unlimited set of shape/length/height combinations that could result in the required volume were possible. The final configuration was optimized by using aerodynamic simulation to optimize the shape, as will be discussed in section 9.0. The resulting shape is based on a modified NACA 67-512

airfoil, with an overall length and height of 1800 and 225 feet, respectively. The envelope is shown on Fig.4.

The envelope contains 121 lifting gas cells, and a heaviness control system that makes it possible to reduce the buoyancy as needed, which will be further described in section 10.0. The structure of the envelope is described in section 11.0.

Gondola

The gondola, or fuselage, is the element in which payload is enclosed, as well as the section in which the flight crew is located throughout the flight. The gondola is not a lift generating element, and its design is only based on the goal of minimizing drag by minimizing wetted surface area while providing enough space for both payload and crew.

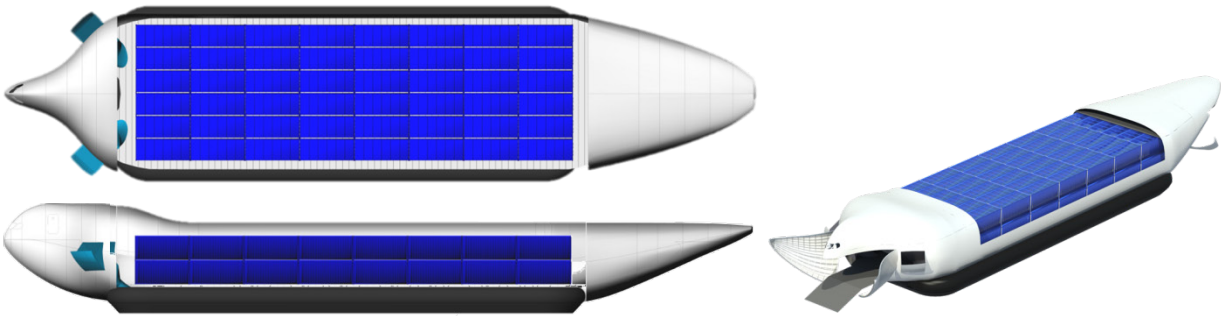

Figure 5. Side, Top and Isometric views of the Gondola in the 96-TEU configuration. Cuts have been made to allow the containers to be seen. Forward and Aft Cargo doors are open and ramps are deployed in the isometric view. The ACLS intakes are also shown.

The requirements presented in the RFP (appendix I) of carrying different types of payloads made it necessary to optimize the shape of the cargo bay to fulfill the requirement while minimizing the area. All the possible cargo distribution configurations where evaluated, taking into account the nature of the items to carry (tanks and helicopters cannot be stacked while containers can). The 96-TEU configuration was the volume-limiting case, and an optimum configuration of 2-6-8 containers high-wide-long was obtained, as shown on Fig. 5.

The crew quarters were designed taking into account the requirement of providing eight-days accommodation for seven crewmembers. These include a cockpit, lavatories, briefing room, kitchen/dining area, and a sleeping/resting area. The crew quarters are located on an upper deck to leave enough space for loading/unloading cargo from the front ramp, as well as to maximize crew safety in case of a hard landing and posterior collapse of the cargo towards the front. Both the crew quarters and the cargo area are air conditioned and oxygenated to enable a personnel-transport configuration.

ACLS

An air cushion landing system was required by the RFP. The design of such system was based on the process described by Yun and Bliault[10]. A bag and finger skirt was selected as it is the type of ACLS skirt most widely used in recent applications. The skirt was sized trying to maximize

the area of the cushion, which minimizes the required pressure and power and increases stability on water. The skirt is located on the lower edges of the payload area, with a length of 50 meters (164 ft.) and a width of 16 meters (52.5 ft.). The system will be further discussed on section 10.0.

Wing Group

As has been previously mentioned, although most of the lift is produced by aerostatic forces, a portion of the lift required by the airship is produced by aerodynamics. The aerodynamic design and optimization showed that in order to minimize drag and fuel consumption, the lift produced by the envelope at cruise altitude should be a very small fraction (around one percent of the total lift). Since buoyancy only represents 90%, wings are required to produce the remaining required lift in an efficient manner.

A three-surface configuration was selected given the limited span available and high lift required, as well as the large moments required to provide sufficient pitch control for the airship to initiate takeoff rotation. Large vertical tails were designed and located on the top back of the envelope, to provide lateral control. The aerodynamic considerations on the designs of the wings are described on section 9.0, the structure on section 11.0, and stability and control are discussed on section 13.0. The wings and the left stabilizer can be appreciated in Fig.6.

Figure 6. Rendered view of the airship in flight.

Final Configuration

Figure 7 shows the final configuration of the airship, including its main dimensions.

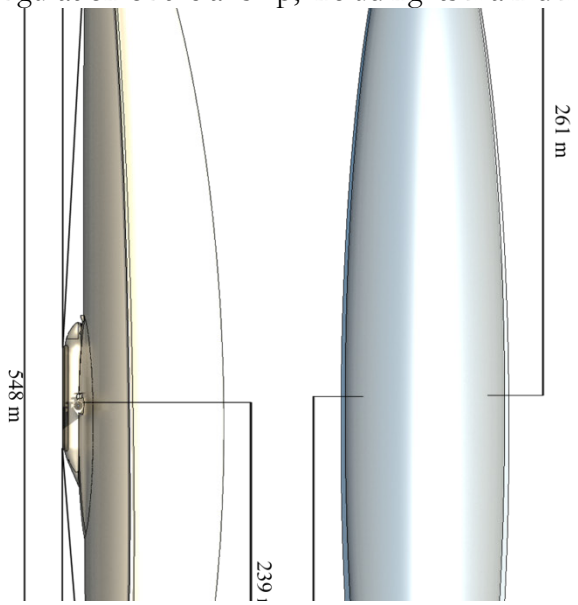

Figure 7. 3-view of the final configuration.

9.0 AERODYNAMICS

Envelope

The aerodynamics of the envelope was one of the most challenging problems to solve for this design. The combination of its low aspect ratio and high Reynolds Number contributed to this difficulty. The $C_{L,env}$ was assumed, considering that because of the envelope's size, it would be sufficiently low to easily achieve the needed amount of lift.

The envelope was divided into 20 longitudinal sections. Assuming a constant C_L, the chords of the sections were found by forcing an elliptical lift distribution. The planform area of each section was calculated by approximating the region between two chords as a trapezoid. Likewise, the volume between two chords was determined by assuming a prism extruded between two ellipses which shared their respective chord's length and equal areas with the longitudinal cross section at those chords. By adding up all the sections, the planform area and volume of the envelope were determined. The wetted area was determined by assuming the envelope was an ellipsoid of equivalent overall length span and thickness of the envelope.

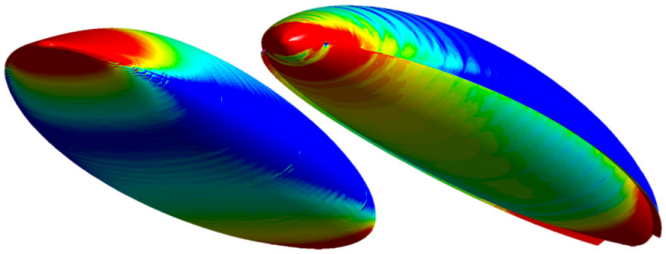

Figure 8. CFD verification of the horizontal fin. Pressure contours shown on the surface, blue low, red high

The drag of the envelope was determined using the standard drag equation:

$$C_{D_0,env} = C_{D,env} + K_{env}{C_{L,env}}^2, \tag{3}$$

Where $C_{D0,env}$ and K_{env} were calculated by the fuselage drag estimation methods given in Roskam [11].

After initial CFD analysis, it was found that this method produced results with significant errors. Additionally, the slender bodies tested produced little to no lift. The slender body lift issue was addressed by adding a long, slender fin along the length of the envelope, as shown in Fig. 8, dramatically increasing lift. The lift of the tested model was improved by a factor of 220, and L/D was increased by a factor of 26. A representative sample of potential envelope shapes were then analyzed using CFD, as shown in Fig. 9, and statistical correction factors were developed using multivariate nonlinear regression methods in MATLAB, using the function nonlinfit. These correction factors are given by Equations 4 and 5.

$$C_{D_0,corr} = 0.841\left(100\,{}^{t}/_{c_{env}}\right)^{-0.1156} {L_{env}}^{-0.0799} {C_{D_0,env,original}}^{0.4978} - 0.0191 + C_{D_0,env,original} \tag{4}$$

$$K_{env,corr} = 0.1376\left(100\,{}^{t}/_{c_{env}}\right)^{1.0594} + 70.9458{K_{env,original}}^{0.1119} - 1.0727{L_{env}}^{0.421} - 61.229 + K_{env,original} \tag{5}$$

The impact of the correction factors can be found in Table 3.

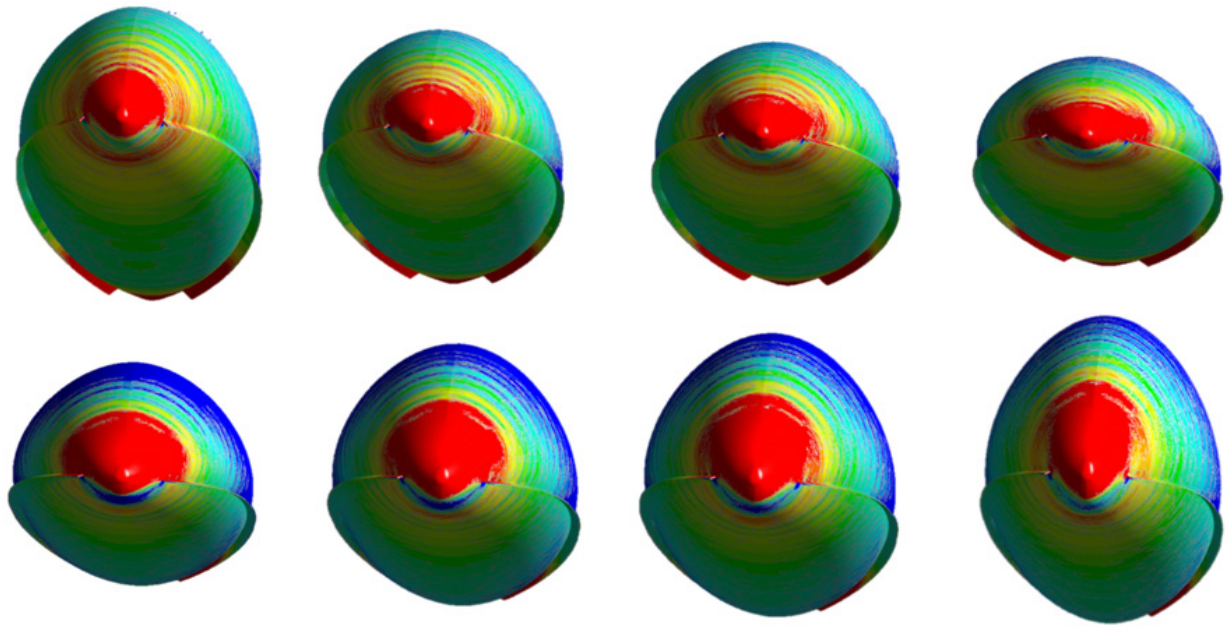

Figure 9 -Array of the 8 configurations tested as the basis for the statistical corrections to the envelope's drag estimation equations.

Table 3. Effect of aerodynamic correction factors on drag prediction of the envelope.

t/c	L (m)	K_{act}	K_{pred}	% Error	K_{corr}	% Error	$CD_{0,act}$	$CD_{0,pred}$	% Error	$CD_{0,corr}$	% Error
10	498	2.12	1.60	-24.38	2.09	-1.52	0.006317	0.003131	-50.44	0.006267	-0.01
10	575	2.67	1.85	-30.75	2.63	-1.45	0.006107	0.003176	-47.99	0.006214	0.02
10	610	2.78	1.96	-29.36	2.86	2.78	0.006362	0.003203	-49.65	0.00623	-0.02
10	705	3.42	2.27	-33.71	3.40	-0.63	0.006407	0.003292	-48.62	0.006364	-0.01
15	407	2.16	1.31	-39.31	2.16	0.09	0.008142	0.003718	-54.33	0.008106	0.00
15	470	2.70	1.51	-44.09	2.71	0.09	0.008066	0.003767	-53.30	0.008037	0.00
15	498	2.92	1.60	-45.03	2.94	0.67	0.008117	0.003800	-53.19	0.008063	-0.01
15	575	3.51	1.85	-47.34	3.48	-0.94	0.008247	0.003913	-52.56	0.008248	0.00

As can be seen in Table 3, the correction factors greatly improve the accuracy of the estimates of envelope drag and allow for a proper exploration of the full design space.

Wings

The wings were treated as traditional aircraft wings and their drag was predicted by the method presented in the wings section of Roskam [11].

Drag Breakdown

A drag breakdown for the airship is shown in Fig. 10. As can be seen, the majority of the drag comes from the envelope and the lifting surfaces, and almost 90% of the drag comes from the envelope. For this figure, the drag of the fuselage was scaled by wetted area from the envelope, and the drag for the vertical tails was scaled by wetted area from the wings. As can be seen, they together make up just 4% of the drag. This justifies their exclusion in the bulk of the analysis.

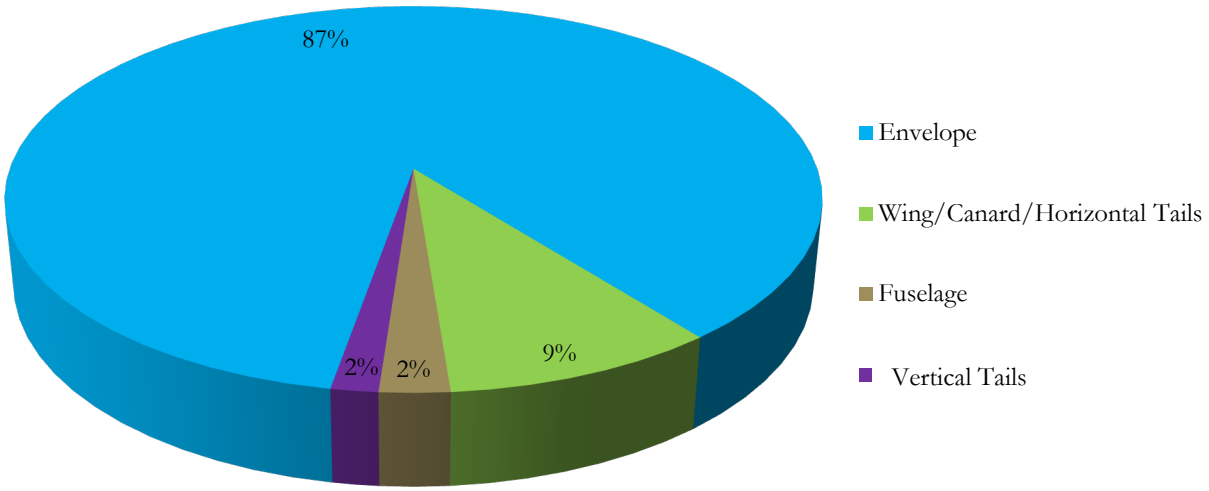

Figure 10 - Drag Breakdown.

10.0 System Integration

In addition to the main structural and functional elements described in section 8.0, the airship includes a group of systems that contribute to the successful operation of the craft. These systems include the ACLS, the heaviness control system, the air conditioning system and the power system; all of which will be described in this section.

ACLS

As stated previously, the airship does not utilize a conventional landing gear system, but instead has an air cushion landing system that allows it to land and take-off from any level surface, including water, snow, and soft unprepared terrains, in the manner hovercrafts do.

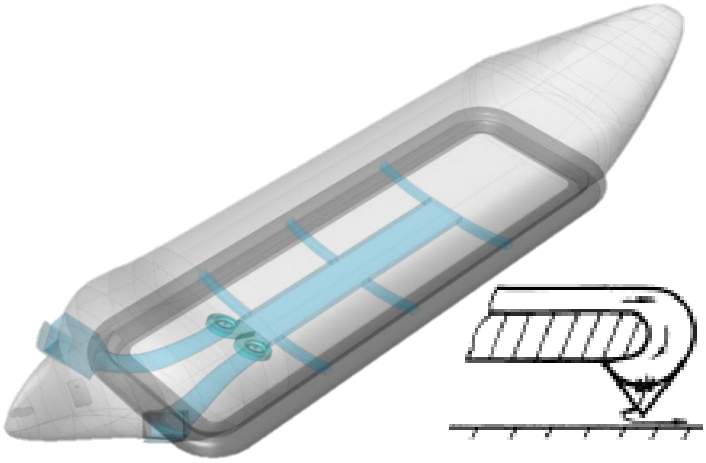

Figure 11. ACLS system in the Gondola. Intakes, fans, and plenum are colored blue. Skirt is colored black. The insert shows the cross-section of the Skirt [10]

Figure 11 shows the designed ACLS in the gondola of the airship. The ACLS system takes air from the atmosphere from two large intakes located on the front of the gondola and compresses it using two fans into a high-pressure plenum, from which it fills the skirt bag. High pressure air then leaves the skirt, generating a middle-pressure "cushion" under the airship, which acts on the bottom of the gondola, producing the lift required to keep the craft from touching the ground. After following the method of Yun and Bliault[10], the ACLS was designed. The main characteristics of the skirt are summarized on Table 4.

Table 4. ACLS System Characteristics

Item	Value
Displacement (Lift)	260,000 lb.
Cushion Length	164 ft.
Cushion Width	52.5 ft.
Hovering Height	0.72 ft.
Cushion Pressure	0.213 psi
Number of Fans	2
Flow Rate per Fan	6070 ft^3/s
Fan Size (Diam./height)	11/1.6 ft.
Total Power Required	1600 hp

The ACLS system improves take-off by supressing wheel-ground friction, and makes it possible for the aircraft to land on any type of terrain. However, special considerations are to be taken for landing operations, since the elimination of surface friction makes it impossible to use brakes. Engine thrust reversing must then be used to come to a complete stop while landing.

HCS (Heaviness Control System)

The weight of the airship varies throughout its operation, due to fuel burn, the loading/unloading of payload, and the need to resist wind forces. This change in weight, along with the change in buoyancy with altitude, makes it necessary to have a heaviness control system capable of modifying the apparent weight (total weight minus aerostatic lift) of the vehicle to a desired value. The apparent weight of the airship would vary from around 260,000 lb. (Full load) to around -1,000,000 lb. (Empty, no fuel) if a HCS was not implemented. The system must be capable of providing a constant apparent weight throughout the mission, and should also be capable of increasing the apparent weight of the airship if required for descent.

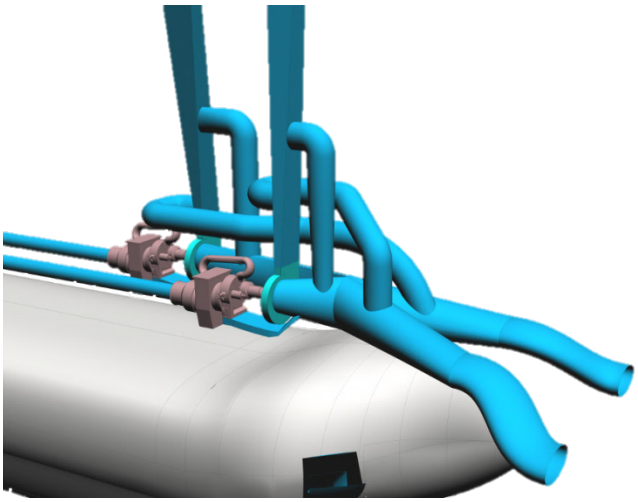

Figure 12. Heaviness control system. Intakes and piping are colored blue. Engines and fans are colored grey

Three compression methods were studied for implementation: High pressure, low volume air compression; high pressure, low volume helium compression; and low pressure high volume helium and air compression. The first two methods consisted on compressing air or helium into small high pressure vessels that would increase the apparent weight of the envelope, which proved to be inefficient and heavy when not in use. The third method, in which air ballonets are inflated inside the envelope and compress the helium cells to a pressure higher than atmospheric pressure, was selected. Additionally, the added air mas further reduces buoyancy. This increase in pressure results in an increased density of the helium inside the envelope and a reduction in buoyancy. There are two fans that take air from the atmosphere and inflate the ballonets inside the envelope to the required pressure to obtain the desired heaviness. The air is re-routed in the opposite direction via large valves and additional ducting to take air from the ballonets into the atmosphere when the opposite effect is desired. Figure 12 shows the piping and fans that drive the heaviness control system. The high complexity of the piping is required for the bi-directionality of the system. Table 5 summarizes the main characteristics of the HCS.

Table 5. Characteristics of the HCS

Item	Value
Number of Fans	2
Total Flow Rate	12360 ft^3/s
Fan Size (Diam./height)	11/1.6 ft.
Power Required	22,000 hp
Maximum Buoyancy Reduction	2,370,000 lb.

Air Conditioning System

The air temperature in both the crew quarters and the payload area is controlled by an air conditioning system. This makes it possible for the airship to transport troops in the cargo bay with some modifications to the interior arrangement. The system is formed by three distributed AC units, each comprising water separators, air heating unit, a heat exchanger, a mixing chamber, an oxygen generator, and temperature controllers, among other components. The cargo area is divided into two zones, each having its own dedicated AC unit. The crew quarters have a single dedicated AC unit; however conditioned air can be redirected to cockpit from other units, if needed.

Power Systems

Besides providing power for flight, the power systems in the aircraft provide power for all the other systems and components. The main sources of power of the airship are six thrust-generating engines mounted on the wings. Each of these engines produces 11,000 hp which can be used to produce thrust via contra-rotating 5.3 m (16.4 ft.) diameter propellers as shown in Fig. 14. The main engines also drive a single high-temperature superconducting[2] (HTS) generators able to generate one megawatt (1340 hp) each. The power from these generators is used for all the electric systems in the airship and to power HTS motors that provide power to the ACLS fans and the lateral thrusters. Two 11,000 hp engines mounted on the upper deck of the Gondola generate the power required for the HCS fans. Figure 13Figure 13. Location of the power systems in the Gondola. Fuel tanks are shown in red. Engines are shown in grey. HTS generators can be seen behind the main engines. ACLS system and thrusters are shown in blue. Violet blocks are EE bays. shows the location of the main power components in the gondola. Figure 155 is a schematic representation of the main systems of the airship.

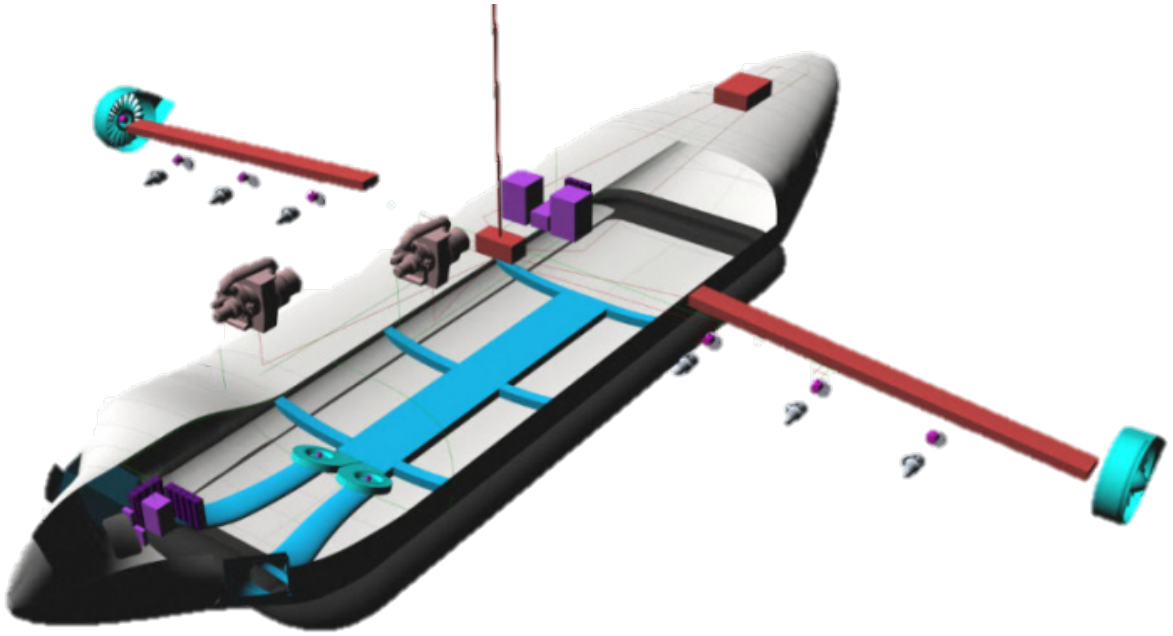

Figure 13. Location of the power systems in the Gondola. Fuel tanks are shown in red. Engines are shown in grey. HTS generators can be seen behind the main engines. ACLS system and thrusters are shown in blue. Violet blocks are EE bays.

[2] Running at temperatures in the range of 50-70 K, far from zero Kelvin.

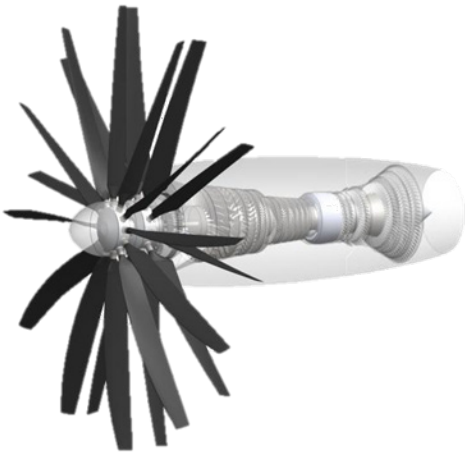

Figure 14. Turboprop engine used in ORCA.

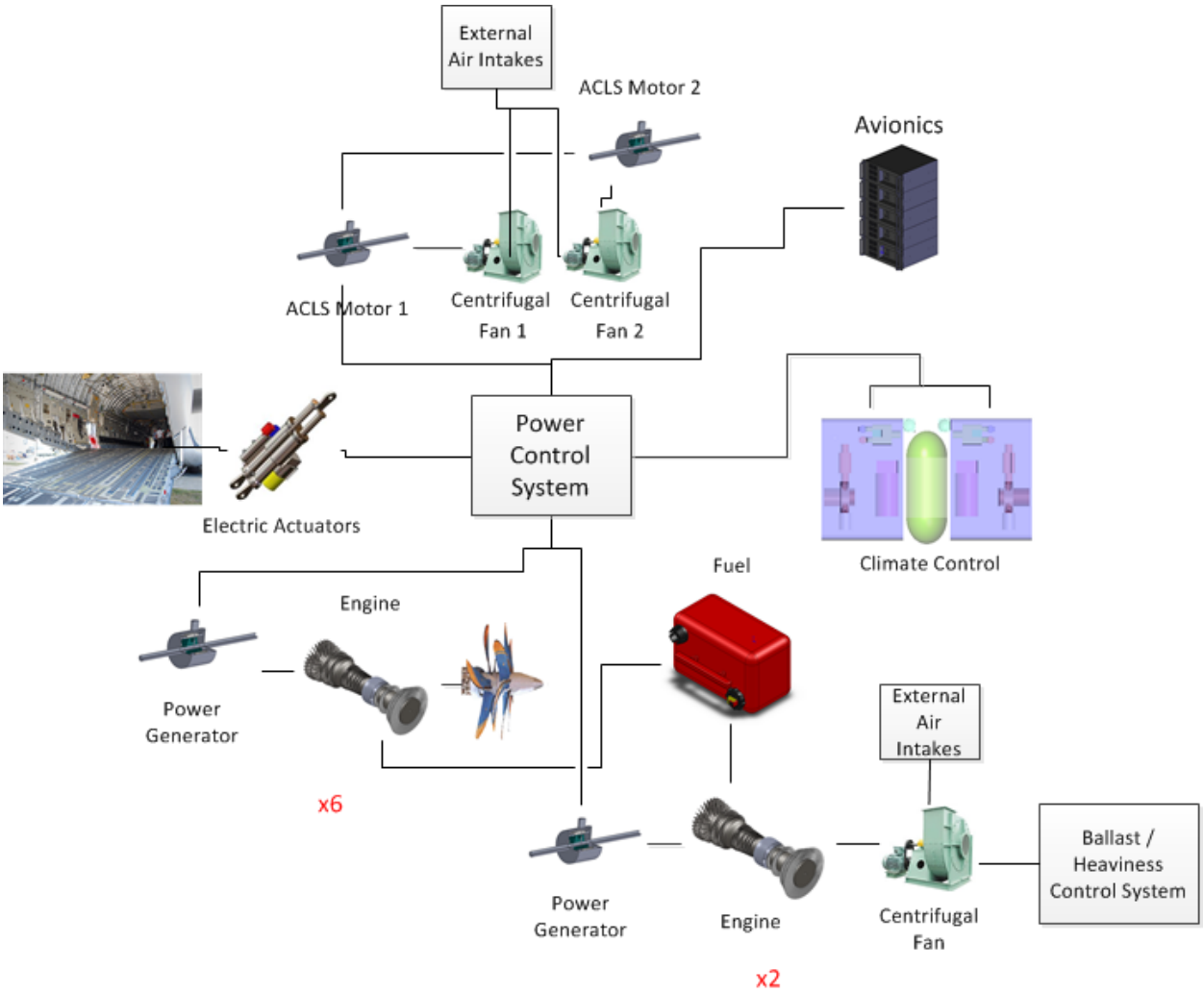

Figure 15. Schematic of the power systems of the Airship

11.0 STRUCTURES

Envelope

The envelope structure was designed by incorporating fundamental physics principles with aerodynamics and materials data. The main engineering challenge was to design the structure so that the very large envelope could support and lift a very heavy payload. The specific issue arose from the lift being distributed over a very long distance, with the load concentrated over a very small area. This challenge was resolved through the initial analysis of existing airship designs, followed by exploration of the design space and further design innovation.

A cable truss structure was designed to handle the large but distributed load throughout the envelope. A lightweight aluminum cable braced keel beam, running the length of the envelope, would serve as a center point to connect the structure of each component together. The center section of the keel beam was required to be rigid and strong enough to support the weight of the gondola beneath it. Two large support cables run along the bottom of the entire envelope and serve to bear the majority of the load and as bracing for the keel beam. The cables vary in diameter according to the load they support, as shown in Fig. 16. The resulting design of the envelope structure is wire braced built around a central keel beam, with two main structural wire bracing cables. The structure is shown in Fig. 17.

The hollow cylindrical aluminum keel beam was designed to be 1800 ft. long and about 6.5 ft. in diameter, with a thickness of only $1/8^{th}$ in. The bending moment induced by the environmental forces (lift and drag), M(x), is calculated from equation 7. The maximum allowable stress, σ_{max}, is a function of the Young's modulus, E, moment of inertia, I, and M(x). Using these factors, the radius of the control beams as a function of x (distance from the center of the keel beam) is found using equation 6. Other parameters used in the calculation are shown in Table 6.

$$r_{cables}(x) = \left(\pm \frac{\sqrt{\sigma_{\max}(2\pi h_{tube}^4 \sigma_{\max} + h_{tube} M(x) - \pi R_{tube}^3 t_{tube} \sigma_{\max})} - 2h_{tube}^2 \sigma_{\max}}{\sigma_{\max}} \right)^{1/2} \qquad (6)$$

Where

$$M(x) = \frac{L_{env}}{2} \frac{x^2}{l_{f,b}} + \frac{D_{env}}{2} h_{drag} x \qquad (7)$$

The radius of the supporting cables is calculated to be about 0.1 in to 4 in, with the radii linearly decreasing with distance x from the center. Longerons and frames brace the skin that surrounds the entire envelope.

Table 6 Structure parameters for calculating the radii of the cables, r_{cables}.

Parameter	Description	Value
σ_{max}	Maximum allowable stress	54.7 psi
L_{env}	Length of the envelope	1800 ft.
h_{tube}	Distance between the centers of the keel beam (tube) and cables	55.8 ft.
R_{tube}	Radius of the keel beam (tube)	3.28 ft.
t_{tube}	Thickness of the keel beam (tube)	1/8th in
D_{env}	Drag of the envelope	7.2x10^4 lbf.
l_f/l_b.	Length of forward/aft beam	840/735 ft.
h_{drag}	Height of the drag	115 ft.
M(x)	Bending moment induced by the environmental forced (lift and drag)	Function of x

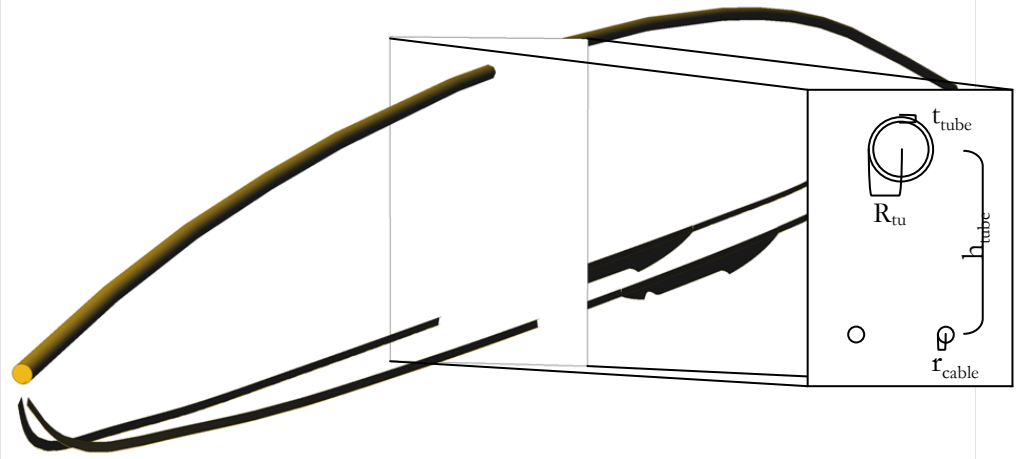

Figure 16. Support cables connected to the center wire-braced keel beam and the gondola help support the majority of the structure.

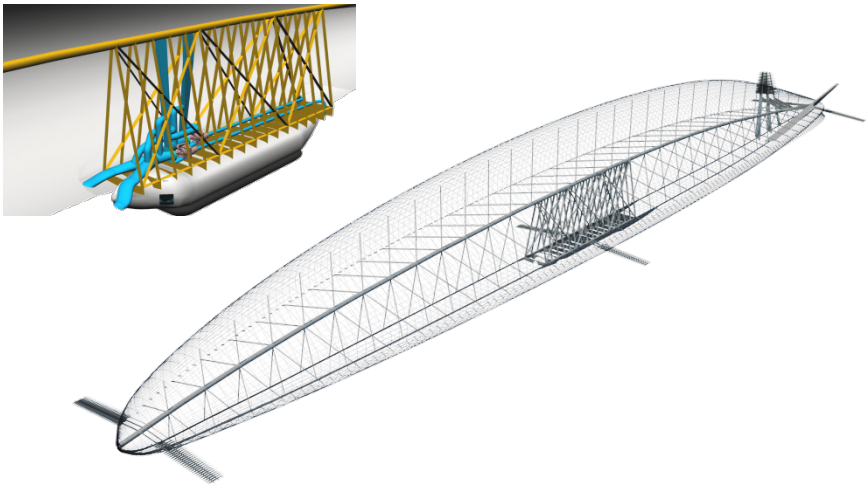

Figure 17. The envelope structure shows the complex arrangement of trusses to support the immense weight of the system. Insert shows detail of gondola connection.

Gondola

The payload-carrying fuselage, or gondola, was designed in accordance with existing aircraft structure design, primarily as detailed in Roskam[12]. Many factors determined the final high fidelity design of the fuselage. Such factors included: pilot and crew safety concerns, significant loads on conventional aircraft fuselage design, the loading and unloading of very large payloads, and climate control and pressurization.

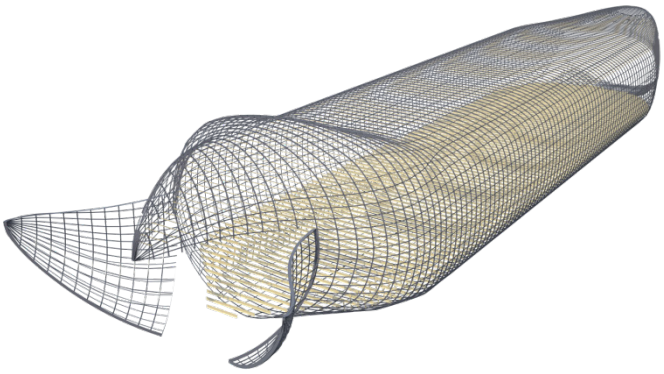

Figure 18. The fuselage (gondola) structure shows a standard large aircraft frame with reinforced floor. Note open front and rear cargo bay doors.

To prevent potential cockpit damage and crew injury from shifting loads in midflight, the cockpit was located safely above the level of the cargo. Additionally, the floor bearing the heavy payload integrates beams that span the width of the deck. These are supported by the frames and on struts, reducing the load on the beams and distributing it on the frames. Thus, there are no concentrated loads on the connection between the frames and the beams. A reinforced ceiling with attached roof cranes makes rapid loading and unloading possible. Special considerations in the ceiling design also allow for ducting for climate control. The fuselage is not pressurized due to the low cruise altitude, cost, and because it is not a necessity. Finally, the cargo bay doors at the front and aft of the fuselage improve the speed and ease of loading and unloading of cargo, as shown in Fig.18. Table 7 shows the design parameters utilized in the fuselage design. Figure 19 shows a cross section of the gondola, with systems and containers in the payload bay.

Table 7. Design parameters of the fuselage structure

Parameter	Value
Frame Spacing	28 in
Frame Depth	2 ½ in
Frame Flange	1 in
Longeron Spacing	15 in
Floor Beam Depth	3 in
Floor Beam Flange Depth	1 in

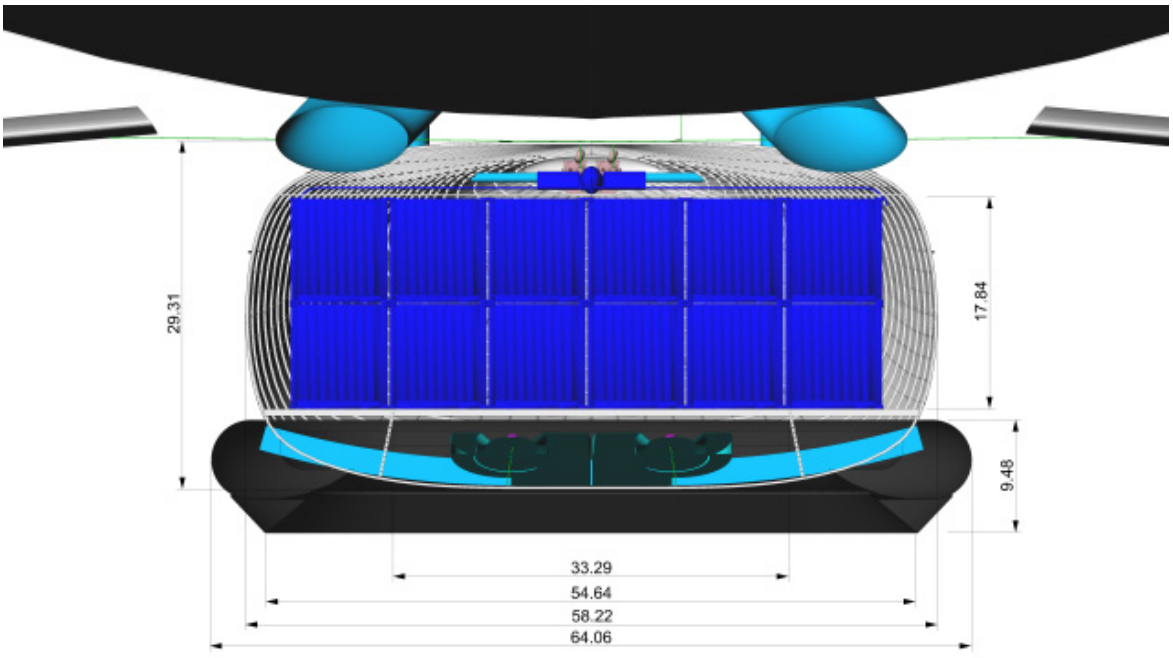

Figure 19. Gondola cross section.

12.0 WEIGHT JUSTIFICATION

The weight of the aircraft was broken down into various groups and the weight of each group was formulated according to statistical models or physical analysis as described in this section. The weight Groups are shown in Fig. 20.

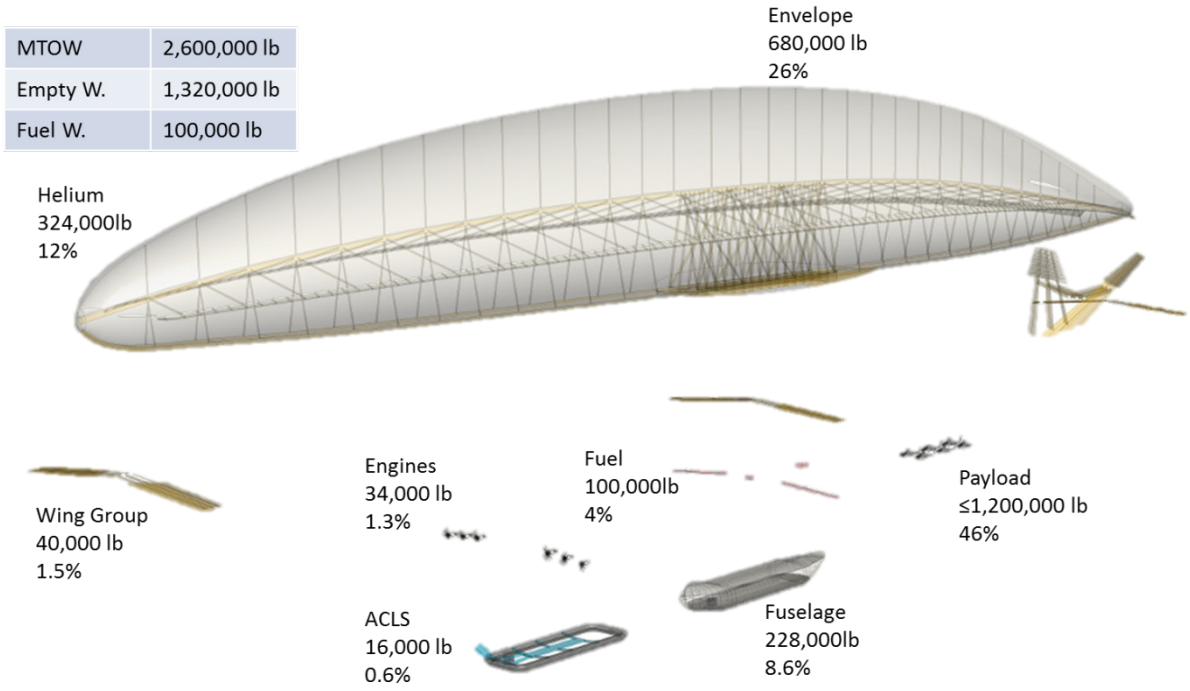

Figure 20. Weight groups. The weight of each group as well as percentage of maximum takeoff weight is indicated next to each item

Payload

The payload weight was assumed to be 1.2 million lb. as specified by the AIAA's RFP.

ACLS

The weight of the air cushion landing system was segregated to account for the weight of the Gearbox and compressors, Electric motors and generators, cryogenic cooling system needed for the operation of the super conducting electric systems, and the skirt. The estimation method proposed by reference 10 was followed. The overall weight of the ACLS system was determined to be 16,000 lb.

Engine

Based on the thrust sizing results, it was determine that six engine will suffice for satisfying all the power requirements. Europrop TP400 engine was selected as the baseline, weighing at approximately 5,700 lb. per unit, including the propulsion system[13]. The total weight of the propulsion group, including pumps, nacelles, and pylons was determined to be approximately 34,000 lb.

Wing

As all the lifting surfaces in the craft were of considerable aspect ratio and wing area, it was determined that the methods for computing the weight of horizontal tails will not apply, and therefore methods presented by Roskam[6] were utilized to estimate the weight of all the lifting surfaces. The total weight of the wing group was determined to be 40,000 lb.

Fuselage

The weight of the fuselage was determined by applying equations presented by Roskam and attributed to the General Dynamics Company for computing the weight of large non-pressurized fuselage structure. It was determined that this group weights at 228,000 lb.

Fuel

The weight of the fuel was computed based on the amount of fuel needed to achieve the endurance and range goal specified by the RFP. The extremely fuel efficient (particularly at lower speed) engines allow the aircraft to accomplish its mission with a 100,000 lb. fuel load, however the maximum amount of fuel is not limited by volume available in the wings, and auxiliary fuel tanks can be added to increase the range and endurance.

Envelope & Helium

The weight of the envelope was computed by accounting for the weight of the structure countering the bending moment of the distributed buoyancy and drag forces acting on the envelope, the pressure vessel structure withstanding the increase in pressure of the envelope to accommodate heaviness control as well as the structure needed to ensure rigidity of the geometry of the envelope.

The formulation of weight for the main load carrying elements of the structure of the envelope is presented previously in the envelope structure. In short, the weight of these elements was computed after the full geometry of the keel beam structure was determined by computing the volume.

The weight of the pressure vessel was computed by simplifying the geometry of the craft to resemble a typical pressure vessel of the same volume with rounded sides for which one can compute the weight based on methods presented by Beer & Johnson[14].

An additional weight component was added to this group to account for rigidity members of the structure, mostly on the surface of the envelope. An area density of 0.5 lb./yd^2 was selected as recommended by Khoury and Gillett[15], and the surface area of the envelope was multiplied to obtain the weight of the rigidity surface members.

The total weight of the envelope structure is approximated at 680,000 lb., and the weight of the helium occupying the envelope is estimated to be 324,000 lb. Table 8 presents a summary of the weight build-up of the ORCA hybrid airship.

Table 8. Weight summary

Item	Weight [lb]
Payload	1,200,000
Wing	40,000
Fuselage	228,000
Fuel	100,000
Propulsion	34,000
Envelope Total	680,000
Helium	324,000
Empty Weight	1,320,000
Max Takeoff Weight	2,600,000

13.0 STABILITY AND CONTROL

As it is general practice for the design of airships, ORCA was designed with a slightly negative static margin of -20 percent of MAC of the central lifting surface to facilitate easier maneuverability in the longitudinal direction[15]. This in turn leads to a vehicle with unstable longitudinal stability, therefore requiring a stability augmentation system which will interact with longitudinal control surfaces of the craft to create an artificially stabilized flight. As the moment of inertia of the craft about the y-axis is expected to be fairly large (estimated at 46,800,000,000 lb-ft^2), and the time constant expected for such a large craft are typically fairly long, no sophisticated flight augmentation with rapid reactions will be required for ORCA.

The horizontal lifting surfaces installed at both ends of the craft are sized to produce enough pitching moment at takeoff condition (TO Rotation speed of 82 ft./sec) to initiate a takeoff rotation with a sustained pitch rate of 0.0523 rad/sec. Although in basic comparison this figure may seem low at first, one must note that as ORCA relies very heavily on buoyancy lift, its takeoff does not feature a large rotation angle. In flight simulations performed, it has been observed that the craft is able to leave the ground with a very low rotation angle.

14.0 PERFORMANCE

Special Considerations

Because of the nature of hybrid airships, the analysis of the airship's performance differs slightly form that of a traditional aircraft, and this will be most evident in the range-payload diagrams. The access to a variable amount of buoyant lift though the heaviness controls system allows for both VTOL and non-VTOL missions, depending on the payload. Insight into the modified equations for hybrid airships was gained from Zhang et al[7].

Range-Payload Diagrams

The range-payload and endurance-payload diagrams can be found in the figures below. The base range exceeds the requirement of 6,000 nmi, at 7646 nmi, because the fuel capacity is sized by the endurance mission. The increased range and endurance in exchange for payload is much greater than that of a traditional aircraft, with a zero payload maximum range of 170,000 nmi, and a zero payload maximum endurance of 81 days.

The low fuel consumption and high payload capacity allows for this great lengthening of range and endurance. Some of this fuel efficiency can be exchanged for the capability of vertical takeoff and landing. In Figs. 21-24, all the area below the blue lines is the VTOL capable area. The blue line represents the maximum payload for VTOL. The short vertical section of the blue line represents the transition from max payload to VTOL max payload by removing payload and not replacing it with fuel. The red line represents the removal of payload the direct substitution by weight with fuel.

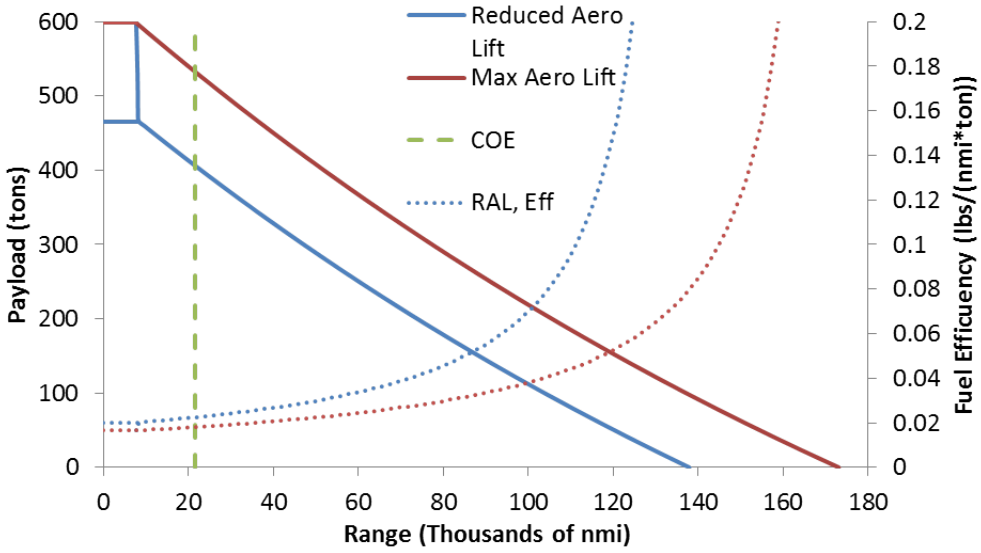

Figure 21. Range payload diagram. A measure of efficiency is shown on the right axis and is plotted with the dotted lines. The green dashed line represents the distance required to circumnavigate earth at the equator

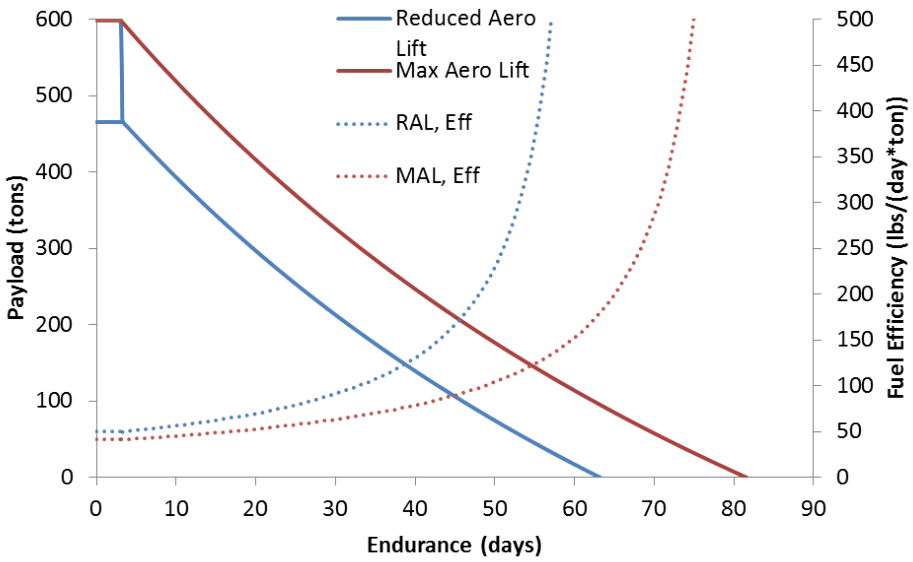

Figure 22. Endurance payload diagram. A measure of efficiency is shown on the right axis and is plotted with the dotted lines.

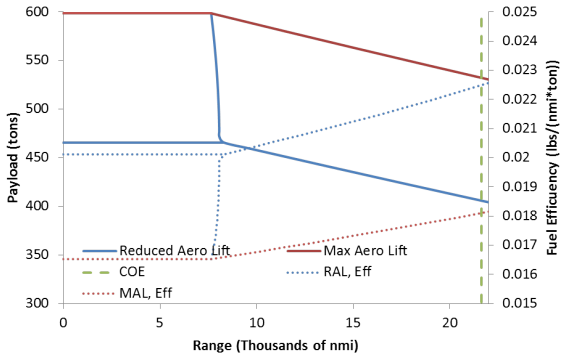

Figure 23. Close up of the low-range region in figure 18

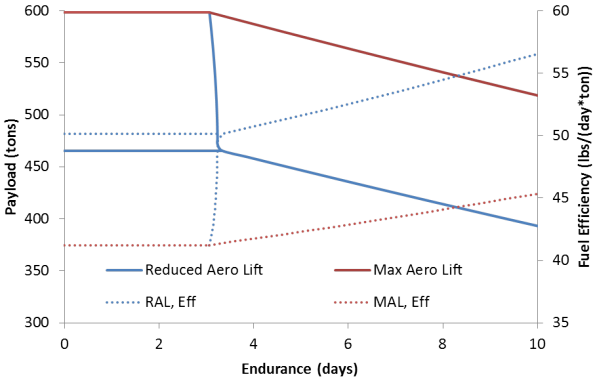

Figure 24. Close up of the low-endurance region in figure 19

15.0 OPERATIONS

Description of a mission

Upon completion of the airship design, and taking into account airport compatibility, infrastructure design, and other special considerations, a mission profile can be described. ORCA is designed to utilize existing airport infrastructure as previously described. Requirements for airport compatibility include a reinforced field or concrete parking area, located near airfreight facilities, for loading, unloading and docking. Additional considerations at feasible airport locations include roadways for transportation of freight.

A typical mission begins with the loading of the cargo through the aft and front of the gondola using the foldable ramps attached at each end. If required, bridge cranes attached to the ceiling of the cargo bay stack the payload in an efficient manner. The cargo is tied down to the reinforced floor. Fuel is loaded according to conventional aircraft standards. It is assumed that the helium has been supplied to the enveloped from a distant source.

After the payload is loaded and secured, ORCA's engines and power systems start and warm up. The large airship then taxis to a cleared runway and takes off. After a relatively long maneuver over the airport, ORCA climbs to 10,000 ft., levels out and cruises toward the destination. The long duration of the cruise period requires three sets of crew rotating in eight-hour shifts. Living quarters and provisions are also provided for the journey. The aircraft begins its descent as an average freightliner toward the final destination.

ORCA maneuvers, descends, and then lands at the distant destination. The very large airship is then taxied to its parking area away from the runway, where it is docked. The unloading is done in much of the same manner as the loading, only in reverse order. The airship then awaits its next mission. Figure 25 and Table 9 describe the mission segments of the regular mission defined for the airship.

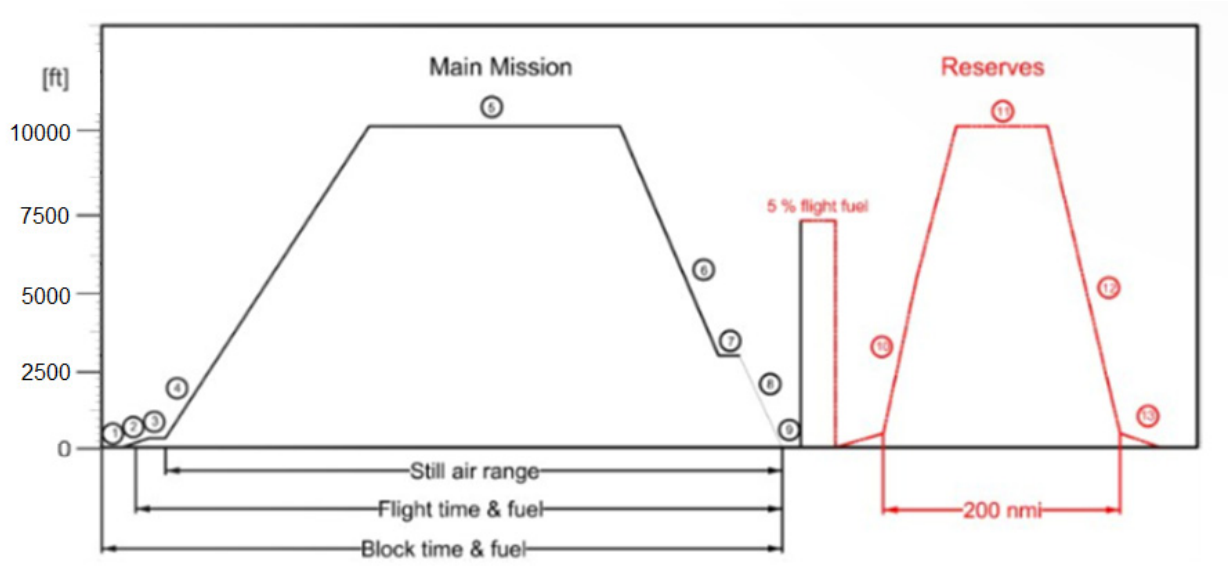

Figure 25. Mission Profile

Table 9. Characteristics of each mission segment

Mission Segment	Altitude (ft.)	Speed (keas)	Vert. speed (ft./min)	Distance (nmi.)	Time (min)
0. Load	0	0	0	0	60
1. Warm Up	0	0	0	0	30
2. Taxi-Out	0	0	0	0	10
3. Takeoff	0	60	0	0.1	2
4. Climb	0 - 10,000	80	1500	8.7	7
5. Cruise	10,000	90	0	6000	57 hours
6. Descent	10,000 - 1,000	80	-300	43	30
7. Loiter	1,000	80	0	0	120
8. Descent	1,000 - 0	70	-300	5	3
9. Land/Taxi	0	50	0	0.1	5
10. Unload	0	0	0	0	45

Airport compatibility

Initial aircraft dimension and weight specifications indicated that either the airship design would require modification or existing airport infrastructure would require major upgrades or changes. Since the payload, range, and cruise altitude requirements are fixed, only modifications to envelope dimensions could be made. Therefore, an analysis of current airport infrastructure and existing large aircraft was necessary for a complete assessment of airship compatibility.

Many factors play a role in the implementation of a new aircraft in existing airports. Such factors include: runway width, length and load capacity, runway signage, taxiway clearance, loading and unloading area clearance, and traffic flow in and out of the airport. As an example, in order to accommodate the 80 m (262 ft.) wingspan of the Airbus A380, JFK International Airport made several extensive changes, including longer and wider runways[16]. Aircraft characteristics highly influence the size and operation of airport facilities.

The weight of the airship is driven by the large cargo load of 1.2 million lb. it must carry. By comparison, the gross weight of an A380-800 is about 1.2 million lb.[17]. In order to determine whether or not current airport runways are able to handle such gross weight, it is necessary to consider runway pavement design. The maximum stress to be used for a reinforced isolation joint (typical of runway pavements) is found using FAARFIELD thickness design software[18]. It is found from the analysis that the B777-300 ER, which contributes a maximum free edge stress for a concrete section of 477 psi, determines the pavement strength[17]. Thus, the ACLS structure, which houses a frame on which the airship rests, must be designed in such a way that the surface it rests on supports no more than 477 psi.

According to the FAA, the maximum installed airport sign height is 42 inches at a minimum 35 feet from the defined payment edge[18]. Also, as stated, the sign height should be reduced, if necessary, to provide the required 12-inch clearance between the top of the sign and the critical aircraft. Thus, the airship's width and height is not determined by runway signage.

Figure 26. The airship's width and length are the main factor in determining airport compatibility. The airport shown is LAX, with scaled airship model and labeled 747.

Other runway factors to consider before an adequate sizing of the airship can be performed are the runway width and length. Due to the 6700 ft. takeoff distance required by the AIAA RFP and the slow approach speed of the airship, the runway length is not an issue at most airports. Runway width, however, is an important factor due to the relatively close proximity to nearby runways and loading and unloading structures, as can be appreciated in Fig. 26. The high wingspan of the A380 (Fig. 27) set the bar for large aircraft compatibility at existing airports. Therefore, in order to utilize the large airports with A380 upgrades, the airships design must incorporate a maximum width of 80 m (262 ft.), which greatly affects many other design parameters as stated previously.

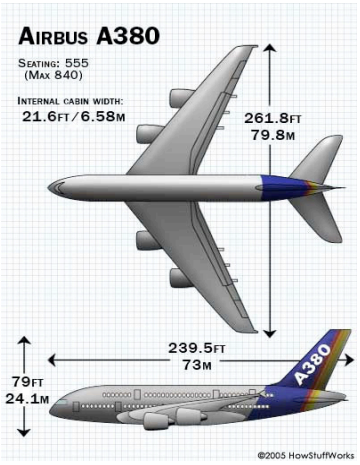

Figure 27. The Airbus A380 set the bar for the width of ORCA

Helium Acquisition

Hydrogen and helium were considered and compared as viable mediums of producing buoyant lift, which accounts for 90% of the total lift of the aircraft. Although not as buoyant as hydrogen, helium was the decided means to create the buoyant lift of the airship because of its nonflammable properties. While once rare and expensive to produce, helium is now an affordable byproduct of natural gas. Through good fortune, helium was found in large quantities under the American Great Plains[19]. This fact enables the United States to be the world's leading supplier of helium, driving down costs for its local use in hybrid air vehicles. Figure 28 shows the historic fluctuation of the helium market.

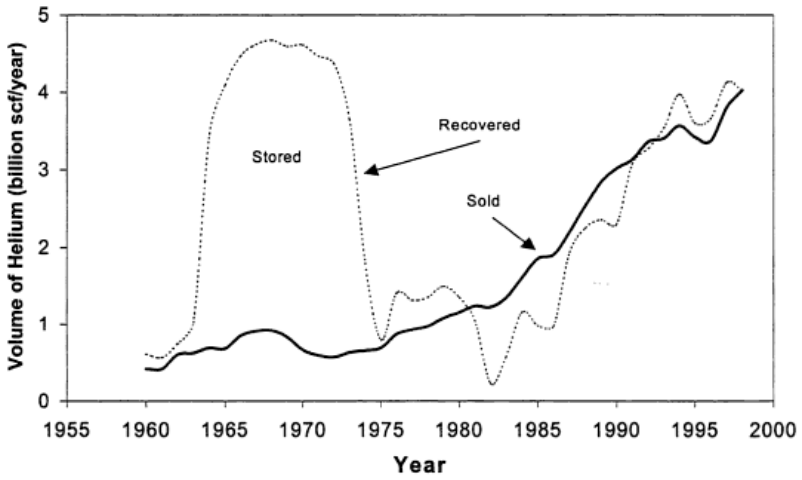

Figure 28. Annual helium recovery and sales, 1960-1997. Source: Bureau of Land Management

The current price of helium was adjusted by the US Government in 2010, and is set at $\$0.075/ft^3$.[20] This results in a total cost to fill the envelope of around one million dollars.

16.0 COST ANALYSIS

In order to ascertain the merit of a new large cargo aircraft, it must be determined whether or not it provides a costs savings, and in the case of a hybrid airship, whether or not this cost savings is enough to justify the craft's slower speed. The cost analysis was done by the method presented by Roskam[8].

While the method is very robust and complete, in order to get accurate results the coefficients of the equations must be filled in appropriately. Some worry is caused in the fact the many of the equations are limited to craft of up to 1,000,000 lb. While the ORCA greatly exceeds this, there is no better method available.

Some examples of these coefficients are easier to obtain, such as the manufacturing labor cost, the number of engines, and the aircraft's weight. The equations also contain less precise coefficients such as "difficulty factor", "CAD factor", and "Overhead Factor". This being said, a significant effort was put forward to make all cost estimates both accurate and conservative. Additionally, all cost data used for comparison was gained by applying the same cost methods to another aircraft, namely the Boeing 747. The data is presented in Table 10.

Table 10 - Cost Summary. Based upon a production run of 100 ORCAs and 400 747s.

Parameter		ORCA	747	Units	Description
CRDTE		7380	16067	$ Millions	R&D, test, and evaluation costs
	Cftor	216.9	920.1	$ Millions	Flight test operations cost
	Cpror	738.0	1607	$ Millions	Profit cost
	Cfinr	738.0	1607	$ Millions	Financing cost
	Caedr	456.3	2421	$ Millions	Cost Engineering and design
	Cdstr	170.0	1503	$ Millions	Cost support and testing
	Cfta	5061	8009	$ Millions	Flight test airplanes cost
CACQ		24167	70378	$ Millions	Acquisition cost
	CPRO	2197	6398	$ Millions	Profit costs
	CMAN	21970	63980	$ Millions	Manufacturing cost
DOC		285.6	99.63	$/nmi	Direct Operating Cost
	DOCflt	52.61	49.27	$/nmi	Flying direct operating costs
	DOCmaint	151.0	28.20	$/nmi	Maintenance costs
	DOCdepr	53.27	13.83	$/nmi	Depreciation costs
	DOClnr	8.722	1.364	$/nmi	Fees/taxes costs
	DOCfin	19.99	6.974	$/nmi	Financing costs
DOC		0.4760	0.5693	$/(ton*nmi)	Direct Operating Cost
	DOCflt	0.08803	0.2804	$/(ton*nmi)	Flying direct operating costs
Fuel Cost		0.0158	0.2091	$/(ton*nmi)	Fuel Cost
AEP		335.6	227.5	$ Millions	Airplane Estimated Price
AMP		746.4	327.6	$ Millions	Airplane Market Price

The data is based on an assumed production run of 100 ORCAs and 400 747s. The DOC in $/(ton*nmi) is lower than that of a 747, but it probably wouldn't be enough to justify this new aircraft, being only a 16% reduction. Here the DOC components, specifically the Maintenance and Depreciation costs, seem unusually high for ORCA. This is most likely because of the large weight of ORCA being outside the weight range for the equations. However, when flying costs (crew, petroleum, and insurance) and fuel costs are compared in $/(ton*nmi), ORCA saves 68% and 92% respectively. ORCA saves money in fuel, but is more expensive in insurance and crew costs. This still results in a large savings overall. Moreover, the equations for DOCflt are less a function of weight than the others. The only way weight is factored in is though the insurance costs, which is based on the AMP, which is a function of weight. Given this, the AMP seems like a reasonable figure, and therefore DOCflt can be trusted. Accordingly ORCA appears to have the potential to be very competitive in the air cargo market.

17.0 CONCLUSIONS

- There appears to be a market demand for a vehicle that is faster than seaborne ships and slower than transonic cargo aircraft. ORCA presents a concept that satisfies all the requirements set by the AIAA in their RFP, presented in appendix I, therefore such a concept is an alternative for large volume commercial and military intercontinental cargo transport.

- In order for the design to be successful, it must be compatible with present day airports. During research, it was determined that construction of new airports or retrofitting of existing ones is an extremely expensive solution, and no cargo transportation business would be inclined to pay the cost of such expensive infrastructural development just to be able to utilize a new type of transport vehicle.

- After the design explorations presented in this document, a vehicle was designed with a max takeoff weight of 2.6 million lb., payload weight of 1.2 million lb., with a length of 548 meters (1800 ft.), a span of 80 meters (262 ft.) and a height of 81 meters (265 ft.), powered by six 11,000 horsepower turboprop engines.

- While carrying its maximum payload, the vehicle has a nominal range of 6,000 nmi, and an endurance of 3 days. The cruise speed is 90 keas, at a cruise altitude of 10,000 ft.

- A mission profile, as well as a generic mission description, is presented for the airship designed.

- The compatibility requirements have defined the configuration of ORCA to a high degree by limiting its span to 80 meters (262 ft.), therefore greatly limiting the number of possible concepts to be explored for further development. .

- A wide range of solutions were evaluated for each system and main component. Trades were made and the finalized configuration was obtained. Main systems include an air cushion landing system, a heaviness control system, and an advanced power system.

- The main physical and performance characteristics of the hybrid airship are presented, which were obtained based on both conventional methods and methods developed specifically for the task.

- A flight simulation model was developed for the airship, which served as a validation tool for the performance, handling, and flight dynamics characteristics of the airship. From the model, satisfactory results were obtained.

- It was determined that the cash operating cost of such craft will be significantly lower than that of any present day commercial jet airplane. For example, the fuel cost per ton nautical mile of ORCA is computed to be lower than a contemporary 747-8F jetliner by a factor of 22, thanks to the efficiency of the advanced turboprop engines, low drag airframe and the very low cruise speed of the craft compared to transonic jet airplane.

- Automated design tools proved to be a fast, cost effective way of solving design problems and reducing uncertainties. The use of computational fluid dynamics and having a fully integrated CAD model of the vehicle allows for fast analysis, correction, and modification of parameters.

18.0 RECOMMENDATIONS

Following areas of the design and analysis of the ORCA concept may be improved in further development:

- Envelope structure can be sized in a more detailed manner to improve the accuracy of the empty weight of the craft. Effects of irregular shape of the gondola must be accounted for to reflect its effect on the weight of the pressure vessel inside.

- The Fuselage weight has to be estimated in more details, as the fuselage includes items not typical for commercial aircraft, such as very large hinging doors, offloading equipment and large roller systems. This will increase the accuracy of the overall weight estimation.

- Although the flight simulation has indicated that the vehicle has reasonable handling qualities in pitch and yaw, the rolling performance is not astute. Development of a powered rolling system, i.e. utilizing rotating thruster fans to provide rolling moment, may be a suitable addition.

- As the geometry of the gondola had a very small wetted area compared to the whole craft (around 3 percent of the total), its aerodynamics have been neglected in the analysis. Performing a CFD analysis that would include the effect of gondola on the overall system performance may assist in obtaining more accurate aerodynamic figures.

It can be noted that the effects of modern structural material have not been accounted for in the weight analysis of this craft due to a lack of precedence for using such material in a very large structure. Hence, developing a more accurate weight model of the craft can improve the accuracy of the analysis significantly.

REFERENCES

1. Bureau of Transportation Statistics, U.S. Department of Transportation. *Freight Transportation: Global Highlights*. 2010

2. U.S. Department of Transportation. Maritime Administration. *Annual Report to Congress*. Fiscal Year 2006.

3. Boeing, "Boeing 747 Family - 747-8 Technical Characteristics." http://www.boeing.com/commercial/747family/747-8_fact_sheet.html (accessed April 20, 2011).

4. Bureau of Labor Statistics, "Import/Export Price Indexes." April 2011. http://www.bls.gov/mxp/ (accessed April 20, 2011).

5. Boeing, "Boeing 747-8 Intercontinental and 747-8 Freighter." http://www.boeing.com/commercial/747family/747-8_facts.html (accessed April 20, 2011)

6. Roskam, Jan. *Aircraft Design*. V, *Component Weight Estimation*. Wichita, KS: DAR Corp, 1986

7. Zhang, Ke Shi et al. "Flight Performance Analysis of Hybrid Airship: Revised Analytical Formulation." Journal of Aircraft 47, no. 4 (2010): 1318-1330.

8. Roskam, Jan. *Aircraft Design*. VIII, *Airplane Cost Estimation*. Wichita, KS: DAR Corp, 1986

9. Wong, J. Y. *Theory of Ground Vehicles*. 2nd Ed. New York: John Wiley & Sons, Inc., 1993.

10. Yun, Liang, & Bliault, Alan. Theory and Design of Air Cushion Craft. 1 ed. London: Arnold Publishing, 2000.

11. Roskam, Jan. *Airplane Design*. VI, *Preliminary Determination of Aerodynamic, Thrust and Power Characteristics*. Wichita, Kansas: 1986.

12. Roskam, Jan. *Airplane Design*. III, *Layout Design of Cockpit, Fuselage, Wings and Empennage*. Wichita, Kansas: 1986.

13. Europrop International. "Europrop TP400 D6". http://www.europrop-int.com/pages/tp400/tp400_d6.htm (accessed April 18, 2011)

14. Beer & Johnson, *Solid Mechanics*. 10th ed. New York: McGraw-Hill, 2006.

15. Khoury, Gabriel & Gillett, J. *Airship Technology*. Cambridge: Cambridge University Press, 1999.

16. Gomes de Barros, A. & Wirasinghe, S. *New Aircraft Characteristics Related to Airport Planning*. First ATRG Conference. Vancouver, Canada, June 25-27, 1997.

17. U.S. Department of Transportation, Federal Aviation Administration. *Airport Pavement Design and Evaluation*. 9/30/2009

18. FAA AC/150/5340-18F

19. National Research Council (U.S.). Committee on the Impact of Selling the Federal Helium Reserve. *The impact of selling the federal helium reserve*.

20. Inter-American Corporation Helium Exploration and Production. *Value of Helium*. http://www.helium-corp.com/facts/heliumvalue.html (accessed April 10, 2011)

Appendix I: Request For Proposal